ARCHIVES OF ELECTRICAL ENGINEERING VOL. 60(4), pp. 519-529 (2011)

DOI 10.2478/v10171-011-0042-3

Wedge functions applied to 2D magnetostatic problems*

ERNST HUIJER, SAMI H. KARAKI

American University of Beirut
PO Box: 11-0236, Beirut, Lebanon 1107 2020
e-mail: {eh09/skaraki}@aub.edu.lb

(Received: 21.06.2011, revised: 30.09.2011)

Abstract: In this paper the application of so called wedge functions is presented to solve two-dimensional simple geometries of magnetostatic and electrostatic problems, e.g. rectangles of varying aspect ratio and with different values of the magnetic permeability μ. Such problems require the use of surface charge density, or segment source, functions of the form $\rho_s = \sigma^{a-1}$, where the power parameters, a, have special fractional values. A methodology is presented to determine these special values of a and use them in segment sources on simple geometries, i.e. rectangles of varying aspect ratio, and with different values of the magnetic permeability μ. Wedge solutions are obtained by coupling the strength coefficients of source segments of the same power around an edge.These surface source functions have been used in the analysis of conducting and infinite permeability structures. Here we apply such functions in a boundary integral analysis method to problems having regions of finite permeability.

Key words: finite permeability, wedge functions, segment functions, boundary integral method

1. Introduction

Analysis of magnetostatic problems in geometries for which no analytical solution is available are often solved with element based methods such as the Finite Element Method [1] or the Boundary Element Method [2]. Such methods usually lead to large problem size. Furthermore in regions around geometric discontinuities like corners it is difficult to obtain accurate solutions. In such regions the remedy would be to increase the density of the mesh elements. A more fundamental remedy is to use local solutions adapted to the geometry that approach an exact solution.

In this respect a semi-analytic method based on multiple expansion series solutions, and known as the multiple multi-pole (MMP) method, was used by Hafner and Ballisti [3]. They

* This is extended version of a paper which was presented at the 8th International Conference on Computation in Electronics, Wrocław, 11-14.04.2011.

used it to treat geometrically complicated two-dimensional linear electrostatic problems having piecewise homogeneous regions with high accuracy and low computation costs. Ludwig [4] discussed criteria to select and place a discrete set of functions of the series expansion to match the boundary conditions at a set of given points. He chose solution functions corresponding to sources placed at some distance from the boundary to avoid singularities. An essential characteristic of this approach is that potentials are described with functions that naturally satisfy Laplace's equation. Olsen [5] used the MMP method to create a simple model to describe the field of a complex set of magnetostatic sources and provide data for a shielding analysis program. The method uses the maximum likelihood estimation technique to calculate the coefficients of spherical and finite length cylindrical multipole sources whose positions have been defined by the user. Multipole and segment functions have been used for two-dimensional geometries [6] and so called wedge solutions were used for propagation problems [7].

In this paper we extend the earlier application of wedge solutions to magnetostatic problems [8] to structures with finite permeability. The issue with such structures is that the power parameter a in the segment source functions, of the form $\rho_s = \sigma^{a-1}$, have special values that depend on the angle of the wedge and the relative permeability of the wedge material. A methodology is presented to determine these special values of a and use them in segment sources on simple geometries, i.e. rectangles of varying aspect ratio and with different values of the magnetic permeability μ. The strength coefficients of source segments of the same power around an edge are coupled to simulate a wedge solution. The same functions were used before in the analysis of infinite permeability structures [9]. Here we implement such functions in a boundary integral analysis method.

2. Wedge solutions in magnetostatics

The so called wedge solutions [7] refer to the solutions of potential and fields in two-dimensional structures with geometry, e.g. as shown in Figure 1. Here we show a geometry with two wedge regions. The angle of the shaded edge region is shown to be $\pi/2$, but the value of the angle is not a limitation in the analysis. In the wedge geometry shown we can represent the magnetostatic potential as an even function given by:

$$V(r,\varphi) = \begin{cases} v_1 r^a \cos(a\phi) & -\Delta\phi_1 < \phi < \Delta\phi_1 \\ v_2 r^a \cos(a(\phi-\pi)) & \Delta\phi_1 < \phi < 2\pi - \Delta\phi_1 \end{cases}. \tag{1}$$

There is also an odd form of the solution using the sine function. From theabove expressionof the potential we can find the tangential field B_φ as:

$$B_\varphi(r,\varphi) = -\mu \frac{1}{r}\frac{\partial V}{\partial \phi} = \begin{cases} \mu_0 a v_1 r^{a-1} \sin(a\phi) & -\Delta\phi_1 < \phi < \Delta\phi_1 \\ \mu_r \mu_0 a v_2 r^{a-1} \sin(a(\phi-\pi)) & \Delta\phi_1 < \phi < 2\pi - \Delta\phi_1 \end{cases}. \tag{2}$$

From the discontinuity of $H_\varphi = B_\varphi/\mu$ at the boundary we obtain the surface charge density

$$\rho_s(r) = a\left[v_2 \sin(a(\Delta\phi_1 - \pi)) - v_1 \sin\left(a\Delta\phi_1\right)\right] r^{a-1}. \tag{3}$$

The radial component of the magnetic field density B_r is similarly given by:

$$B_r(r,\varphi) = -\mu \frac{\partial V}{\partial r} = \begin{cases} \mu_0 a v_1 r^{a-1} \cos(a\phi) & -\Delta\phi_1 < \phi < \Delta\phi_1 \\ \mu_r \mu_0 a v_2 r^{a-1} \cos(a(\phi - \pi)) & \Delta\phi_1 < \phi < 2\pi - \Delta\phi_1 \end{cases}. \tag{4}$$

By requiring continuity of both quantities $B_\varphi(r, \varphi)$ and $V_\varphi(r, \varphi)$ on the boundary we obtain the equation:

$$\mu_r = \cot\left[a\left(\Delta\phi_1 - \pi\right)\right]\tan\left(a\Delta\phi_1\right). \tag{5}$$

Similarly when $V_\varphi(r, \varphi)$ is odd with respect to φ we obtain:

$$\mu_r = \tan\left[a\left(\Delta\phi_1 - \pi\right)\right]\cot\left(a\Delta\phi_1\right). \tag{6}$$

Given the values of μ_r and $\Delta\phi_1$, we can find a set of values of the parameter a numerically, which are usually fractional values. For some values of $\Delta\phi_1$ these equations may give indeterminate results for μ_r, which may happen when $V(r, \Delta\phi_1) = 0$. The coefficients v_1 and v_2 are not directly coupled anymore through the continuity of V, but coupled through the continuity of B_φ. In this case we obtain integer values of a.

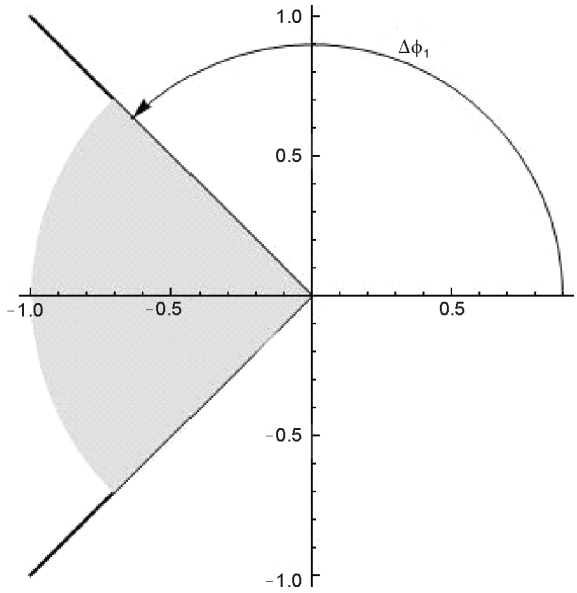

Fig. 1. Wedge geometry with two regions

For example with $\Delta\phi_1 = 3\pi/4$ and $\mu = 100$, the first eight values of a for even and odd potential respectively are:

0.6739, 2.0, 3.3261, 4.6739, 6.0, 7.3261, 8.6739, 10.0
1.3261, 2.6739, 4.0, 5.3261, 5.6739, 8.0, 9.3261, 10.6739.

Examples of wedge solutions for with $\Delta\phi_1 = 3\pi/4$ and $\mu = 100$ are shown in Figures 2-4. Figure 2 shows the plots of the potential $V(r, \varphi)$, and the components of the magnetic field intensity $B_\varphi(r, \varphi)$ and $B_r(r, \varphi)$ at a radius $r = 1$ versus the angle φ, for $a = 0.6739$. And Figure 3 show the same quantities for $a = 1.3261$. Figure 4 shows the variation of the surface charge density with the radius (r) on one of the wedge sides for different values of a.

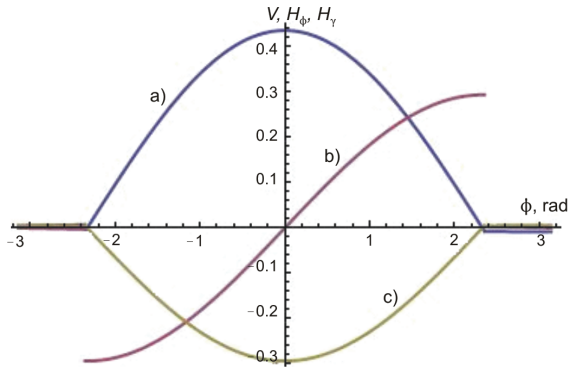

Fig. 2. Potential: a) tangential field, b) and radial field, c) for $a = 0.6739$

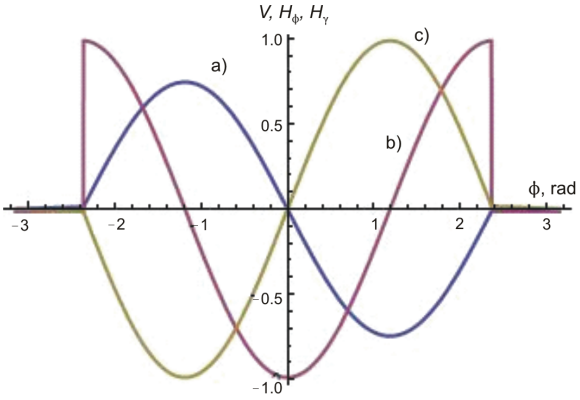

Fig. 3. Potential: a), tangential field, b) and radial field, c) for $a = 1.3261$

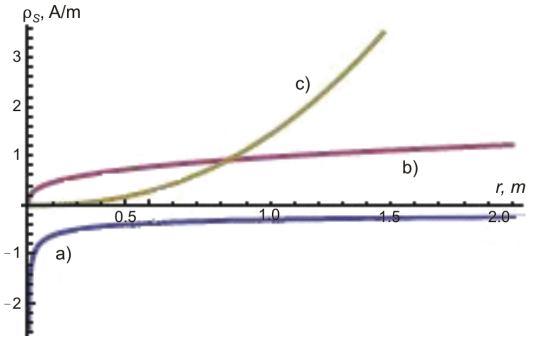

Fig. 4. Surface charge density: a) for $a = 0.6739$, b) for $a = 1.3261$, and c) for $a = 3.3261$

3. Magnetic potential and field expressions

To find the potential at any point (x, y) in space due to a (fractional power a) source distribution of charge density σ^{a-1} on a finite length segment from $\sigma = -l/2$ to $\sigma = -l/2$, we must evaluate the following integral:

$$\mathcal{J}(\sigma, a, x, y) = \frac{-\mu_0}{4\pi} \int \sigma^{a-1} \ln\left[(x-\sigma)^2 + y^2\right] \mathrm{d}\sigma. \tag{7}$$

Mathematica generates the following solution:

$$\mathcal{J}(\sigma, a, x, y) = \frac{-\sigma^a \mu_0}{4\pi a^2} \times$$

$$\times \left(\frac{\sigma_2 F_1\left(1, 1; 1-a; 1 - \dfrac{\sigma}{\sigma - x + \mathrm{i}y}\right)}{-\sigma + x - \mathrm{i}y} + \frac{\sigma_2 F_1\left(1, 1; 1-a; \dfrac{x + \mathrm{i}y}{-\sigma + x + \mathrm{i}y}\right)}{-\sigma + x + \mathrm{i}y} + a \ln\left((\sigma - x)^2 + y^2\right) \right), \tag{8}$$

where ${}_2F_1(\ldots)$ is the hyper-geometric function. From the above function, we can find potential and field expressions that inherently satisfy Laplace's equation. The potential at (x, y) is obtained from evaluation of the definite integral over the length of the segment given by:

$$v(x, y) = \mathcal{J}\left(\frac{l}{2}, a, x, y\right) - \mathcal{J}\left(\frac{-l}{2}, a, x, y\right). \tag{9}$$

The x- and y-components of the corresponding magnetic field are obtained by differenttiating the potential with respect to x and y, respectively:

$$h_x(x, y) = -\frac{\partial v(x, y)}{\partial x} \tag{10}$$

and

$$h_y(x, y) = -\frac{\partial v(x, y)}{\partial y}. \tag{11}$$

The above expressions will be evaluated at points in space along segments defining the geometry of a given object. They represent the fields due to a source segment centred horizontally at the origin (0, 0).

4. Model development

Consider the problem of a magnetic bar of relative permeability μ_r standing in free space. It is required to determine the magnetic field at any point (x, y) in space due to an externally

applied field and the magnetic polarization of the bar itself. The geometry of the bar is defined by 8 segments (s_j with $j = 1, ..., 8$) as shown in Figure 5. Each segment features 8 sources, with each source modelled by a function $\sigma_j^{a_i-1}$ of fractional powers $a_i - 1$, $i = 1, ..., 8$ with 4 values taken from the "even" list and 4 values taken from the odd list. The surface charge, or pole, density on a segment k is described by 8 sources and is given by:

$$\rho_s(\sigma_k) = \sum_{i=1}^{8} c_{ki}\, \sigma_k^{a_i-1}, \tag{12}$$

where σ_k is the metric variable running along segment k, and c_{ki} is the strength coefficient of source i on segment k. The surface pole density which is the normal component of the magnetization is related by the constitutive equation given as:

$$\rho_s(\sigma_k) = (\mu_r - 1) H_\perp(\sigma_k), \tag{13}$$

where $H_\perp(\sigma_k)$ is the total normal magnetic field on segment k at σ_k, which is equal to the sum of the normal magnetization field $H_{\perp\rho}(\sigma_k)$ due to all sources and the externally applied excitation $H_{\perp\mathrm{ex}}(\sigma_k)$:

$$H_\perp(\sigma_k) = H_{\perp\rho}(\sigma_k) + H_{\perp\mathrm{ex}}(\sigma_k). \tag{14}$$

The normal magnetization field is given by:

$$H_{\perp\rho}(\sigma_k) = \sum_{j=1}^{8} \sum_{i=1}^{8} c_{ji} h_{\perp ji}(\sigma_k), \tag{15}$$

where $h_{\perp\mathrm{ji}}(\sigma_k)$ is the normal field to segment k at σ_k due to source i of segment j. This normal field is calculated from its x- and y-components as given by (10) and (11) but rotated and shifted to reflect the position of the source segment with respect to the standard position as described in the previous section. Then x and y have to be evaluated on segment k through functions $x = \mathfrak{g}_x(\sigma_k)$ and $y = \mathfrak{g}_y(\sigma_k)$, as obtained from the geometry of the problem. The above expressions (i.e., 12, 13, 14 and 15) can now be combined as:

$$\frac{\sum_i c_{ki}\sigma_k^{a_i-1}}{\mu - 1} - \sum_j \sum_i c_{ji} h_{\perp ji}(\sigma_k) = H_{\perp ex}(\sigma_k). \tag{16}$$

We can write this equation for every segment k. The left hand side depends on the coefficients c_{ji} and the right hand side on the excitation field.

By applying 4 Legendre polynomial transforms of order $r = 0, 1, 2, 3$ over σ_k to the two sides of equation (16) we obtain 32 (4 × 8) equations. The number four is chosen to obtain the same number of equations as there are unknowns. Note here that the 64 coefficients c_{ji} are reduced by a factor of two due to the source function coupling since coefficients of the same power (a – 1) source on either side of a wedge are equal. So a system of 32 × 32 is obtained, with further reductions possible due to symmetry. For the low aspect ratio rectangle shown in Figure 5 the system size is further reduced by a factor of 4 due to symmetry giving a size of 8 × 8. The column indices j and i in c_{ji} are reshaped as one index $n = 1, ..., 8$ so as to obtain c_n,

and similarly the row indices k and r are reshaped into a single index m = 1, ..., 8. Equation (16) yields the following linear system of equations with c_n being the unknowns:

$$\sum_{n=1}^{8} F_{mn}\, c_n = G_m \quad \text{with } m = 1,...,8, \tag{17}$$

where F_{mn} are Legendre polynomial transforms of the LHS function over σ_k taking in consideration the wedge coefficient coupling and the effect of symmetry; G_m are Legendre polynomial transforms of the RHS of equation (16).

5. Results

As a demonstration of the method we show the analysis results of magnetic two-dimensional bars having rectangular cross-section with relative permeability of 100. We have run cases for varying aspect ratio. In Figure 5 we show the geometry with the segments S1 to S8. This pattern is suitable for rectangles of moderate aspect ratio. On each of the segments, adjacent to a vertex with angle $\pi/2$ we define the surface pole density basis functions, as σ^{a-1}, with $\sigma = 0$ at the vertex and with $a - 1$ equal to the values mentioned before.

In Figure 6 we show the surface charge density, or pole distribution, for a rectangle with aspect ratio 2.5 while going around the circumference as a response to a unity uniform applied field, both in the longitudinal and transverse directions. On each segment we defined four even and four odd source functions.

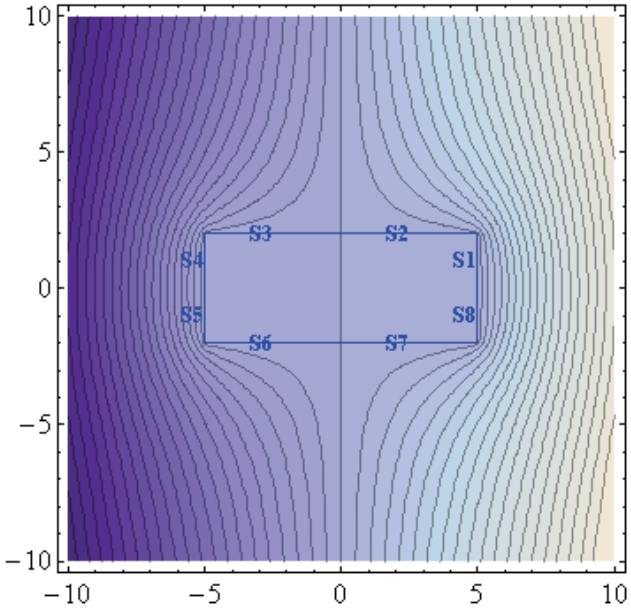

Fig. 5. Equipotential lines of a region of low aspect ratio (2.5) with a longitudinally applied field

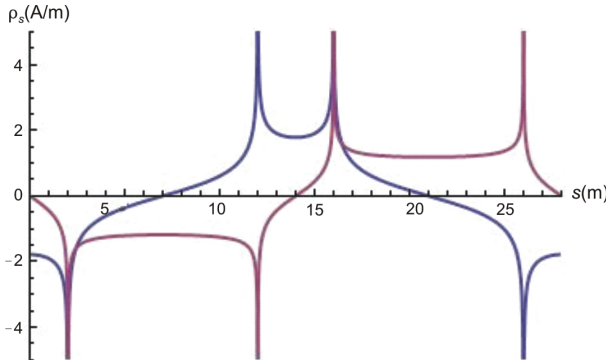

Fig. 6. Pole distribution for region of low aspect ratio

As a measure of error we look at the expression on the LHS of equation (16) where we substitute the solution of the coefficients c_{ji}, expanded into its Legendre's components. The first four components (orders 0 to 3) should match exactly the corresponding values of the excitation field, which in the present examples is either 1 or 0. Higher order Legendre's components are measures of the boundary expression (BE) errors, which are shown in Table 1 and noticeably depicting small values when compared to the excitation value of a unity applied field. When the number of source functions is increased to 12 (i.e. 6 odd and 6 even), then the largest error, corresponding to the Legendre's polynomial of order 6 on segment S2 for the transversely applied field, becomes 2.1793×10^{-5}. This is an order of magnitude lower than the largest error on the same segment of 3.936×10^{-4} when 8 functions are used (Table 1). Furthermore, when 4 functions are used, then the largest error increases to 8.069×10^{-3}. This shows that the method is converging to a more accurate solution as we increase the number of source functions.

Table 1. Residual errors: aspect ratio 2.5

	Longitudinally applied field		Transversely applied field	
Order	S1	S2	S1	S2
4	-1.091×10^{-4}	-3.765×10^{-4}	1.067×10^{-4}	3.936×10^{-4}
5	3.262×10^{-5}	-9.909×10^{-5}	-3.087×10^{-5}	1.176×10^{-4}
6	-5.546×10^{-6}	2.163×10^{-5}	5.033×10^{-6}	-1.666×10^{-5}
7	9.407×10^{-7}	-2.071×10^{-6}	-8.284×10^{-7}	2.539×10^{-6}
8	-1.592×10^{-7}	6.752×10^{-7}	1.369×10^{-7}	-6.235×10^{-7}
9	2.629×10^{-8}	-4.111×10^{-8}	-2.219×10^{-8}	7.644×10^{-8}

With increasing aspect ratio the error increases and it helps to include extra segments on each of the long sides. The number of additional segments needed depends on the aspect ratio, and for the rectangle with aspect ratio 8 two extra segments are needed. On these extra segments we include source functions with a-values of 1/2, 3/2, 5/2 and 7/2, which are obtained by solving a degenerate wedge of angle $\Delta\phi_1 = \pi$. The equipotential lines for long-

itudenally applied field are shown in Figure 7, and the pole distribution is shown in Figure 8 for longitudinally and transversely applied fields. The errors on segments S2 and S3 for these cases are shown in Table 2. The values show that the errors are of the same order as those of the low aspect ratio cases. The errors on segment S1 are an order of magnitude lower than those of segment S2.

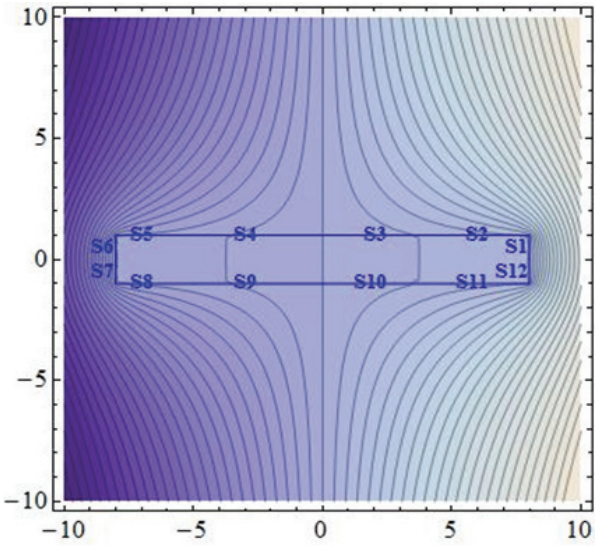

Fig. 7. Equipotential lines of a region of aspect ratio 8 × 1 and an applied field in the longitudinal direction

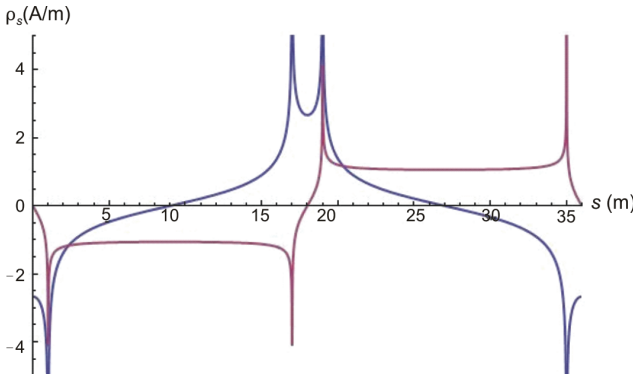

Fig. 8. Pole distribution for a rectangular region: aspect ratio 8 × 1

For an aspect ratio of 64 the same segment configuration yields errors as shown in Table 3. The BE errors are of the order of 10^{-3} and are still small compared to the applied field, nevertheless they are significantly larger than in the previous case of aspect ratio 8. This is used as

an indication to include more segments on the long sides or to use more source functions. And the surface pole density is shown in Figure 9.

Table 2. Residual errors: aspect ratio 8

	Longitudinally applied field		Transversely applied field	
Order	S2	S3	S2	S3
4	-1.178×10^{-3}	2.003×10^{-4}	6.556×10^{-4}	-1.355×10^{-5}
5	-4.090×10^{-4}	-3.649×10^{-5}	2.322×10^{-4}	1883×10^{-5}
6	5.033×10^{-5}	1.398×10^{-5}	-2.653×10^{-5}	-1.015×10^{-5}
7	-1.158×10^{-5}	-3.343×10^{-6}	6.070×10^{-6}	3.103×10^{-6}
8	2.648×10^{-6}	7.761×10^{-7}	-1.463×10^{-6}	-7.522×10^{-7}
9	-4.729×10^{-7}	-2.019×10^{-7}	3.108×10^{-7}	1.758×10^{-7}

Table 3. Residual errors: aspect ratio 64 × 1

	Longitudinally applied field		Transversely applied field	
Order	S2	S3	S2	S3
4	-2.498×10^{-3}	6.958×10^{-4}	6.506×10^{-4}	-1.716×10^{-3}
5	-8.686×10^{-4}	-8.985×10^{-4}	2.315×10^{-4}	2.851×10^{-3}
6	1.061×10^{-4}	1.160×10^{-3}	-2.613×10^{-5}	-2.233×10^{-3}
7	-2.469×10^{-5}	-1.006×10^{-3}	5.715×10^{-6}	1.290×10^{-3}
8	5.594×10^{-6}	8.121×10^{-4}	-1.531×10^{-6}	-6.651×10^{-4}
9	-9.933×10^{-7}	-4.240×10^{-4}	3.022×10^{-7}	2.821×10^{-4}

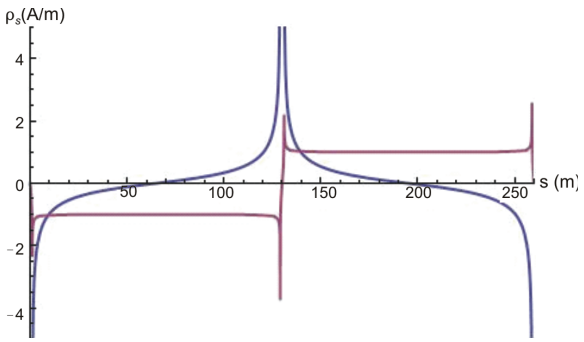

Fig. 9. Pole distribution for a rectangular region: aspect ratio 64 × 1

6. Conclusions

The use of wedge functions has been investigated to solve two-dimensional simple geometries magnetostatic and electrostatic problems, e.g. rectangles of varying aspect ratio and with finite values of the magnetic permeability μ. Such wedge solutions contain surface pole

distributions with fractional power. A methodology has been presented to determine the special values of these fractional powers. Results have shown that very good accuracy of the solution is achieved by solving a linear system of moderate size. A residual error measure was presented to identify whether the system model is adequate or needs further source elements or sources.

Finally one should note that the method is readily extendable to arbitrary magnetic structures with suitable division of the boundary geometry into segments. The method shows promise in reducing problem size in linear magnetostatic computation, as in motors and transformers operating in the linear region of the *B-H* curve, and by extension in computation of physical systems that are governed by equations of the same form, such as electrostatic and electrical conduction systems.

Acknowledgements

The funding of this research by the University Research Board of AUB is gratefully acknowledged

References

[1] Silvester P.P., Ferrari R.L., *Finite Elements for Electrical Engineers* (2nd ed.), Cambridge University Press, pp. 36-47 (1991).
[2] Bätchold M., *Efficient 3D Computation of Electrostatic Fields and Forces in Microsystems*, PhD Thesis No. 12165, Swiss Federal Institute of Technology, Zurich, pp. 20-39 (1997).
[3] Hafner Ch., Ballisti R., *The Multiple Multipole Method (MMP).* The International Journal for Computation and Mathematics in Electrical and Electronic Engineering 2(1): 1-7 (1983).
[4] Ludwig A.C., *The Generalized Multipole Technique.* Computer Physics Communications 68: 306-314 (1991).
[5] Olsen R.G., Lyon C.E., *Modeling of extremely low frequency magnetic field sources using multipole techniques.* IEEE Transactions on Power Delivery 11(3): 1563-1570 (1996).
[6] Huijer E., Karaki S.H., Malkoun J., *Line segment pole functions in the MMP method applied to shielded cables*. IEEE Trans. Power Del. 21: 2082-2087 (2006).
[7] Meixner J., *The behavior of electromagnetic fields at edges.* IEEE Transactions on Antennas and Propagation 20: 442-446 (1972).
[8] Huijer E., *Application of the boundary series method with edge function to magnetic structures of infinite permeability*. SMM19 (Soft Magnetic Materials) Conference, Torino, Italy, 7 September (2009).
[9] Huijer E., *2D Analysis of parallel conductors with polygon shape using special boundary segment functions.* ASM (Applied Simulation and Modelling) 2009 Conference in Palma de Mallorca, Spain on 9 September (2009).